Proc. of the European Safety and Reliability Conference (ESREL 2026)
Edited by José C. Matos, Paulo B. Lourenço, Michael Beer, Daniel Oliveira, Edoardo Patelli, Hélder S. Sousa, Rui A. Silva and Monica Santamaria
 Published by Research Publishing, Singapore.
doi: 10.3850/ESREL2026061419_esrel26-p30221-cd

A Foundation-style Lithium-ion Battery Degradation Model with Varying Operating-Condition Adaptation

Zirong Wang

Department of Industrial Engineering and Management, Shanghai Jiao Tong University, China. E-mail: lcl740308@sjtu.edu.cn

Zhen Chen

Department of Industrial Engineering & Management, Shanghai Jiao Tong University, China. E-mail: chenzhendr@sjtu.edu.cn

Ershun Pan

Department of Industrial Engineering & Management, Shanghai Jiao Tong University, China. E-mail: pes@sjtu.edu.cn

Accurate prognostics of lithium-ion batteries is essential for the reliability and safe operation of battery system, yet facing challenges brought by nonlinearity of capacity degradation trajectories, noise and sensitivity to dynamic operating conditions such as temperature and charge/discharge profiles. To this end, this paper presents a foundation-style degradation modelling framework that learns shared degradation patterns from historical capacity trajectories and then adapts efficiently to a new cell using its early-cycle observations together with the corresponding operating conditions. The proposed model combines a flexible data-driven degradation backbone with a physics-guided operating-condition adaptation mechanism, enabling robust extrapolation under varying conditions while retaining strong expressive capability. A practical pre-training and adaptation pipeline is established to support capacity forecasting and remaining useful lifetime (RUL) prediction for unseen cells. Experiments on CycleLife-SJTUIE dataset from our lab demonstrate that the proposed approach achieves superior capacity forecasting accuracy compared with several baselines and yields lower RUL prediction errors across multiple cells and evaluation metrics.

Keywords: Degradation modelling, RUL prediction, lithium-ion battery, operating-condition adaptation.

1. Introduction

Recent years have witnessed the pervasive deployment of lithium-ion batteries in electric mobility and grid-scale energy storage, where health assessment and lifetime prediction are central to reliability, safety, and life-cycle cost (Zubi 2018). In engineering practice, battery end-of-life is often defined when the capacity degrades to 80% of the nominal capacity (Severson 2019), so modelling the capacity degradation trajectory and extrapolating the RUL are fundamental tasks in battery reliability analysis (Patrizi 2024). However, real-world capacity trajectories are typically nonlinear and stochastic, and they are continuously perturbed by dynamic operating conditions such as temperature, charge/discharge rate (C-rate), and depth of discharge (DOD) (He 2023). This coupling of complex degradation behaviors, time-varying conditions, and measurement noise makes it challenging to build a model that is both accurate and able to generalize across operating conditions (Chen 2024).

Existing studies on capacity degradation and RUL prediction can be broadly grouped into two categories: data-driven methods and model-based methods (Zhao 2023). Data-driven approaches, ranging from conventional regression to deep learning, learn degradation patterns directly from historical trajectories and then extrapolate future capacity and lifetime. Guirguis et al. (Guirguis 2024) proposed a Transformer-based framework for battery state-of-health estimation, achieving superior accuracy

by effectively capturing temporal dependencies and feature-level patterns in battery degradation data. Li et al. (Li 2024) constructed a hybrid data-driven RUL prediction approach for nonlinear and non-smooth capacity trajectories by combining several neural networks and transfer learning. They can deliver strong in-sample accuracy when training data are abundant and the operating condition is relatively stable. However, most transfer-learning or pretrain-and-finetune prognostics models transfer a deterministic feature representation, predictor, or network initialization, and the adaptation stage mainly refits the target-cell observations. The influence of cycle-wise varying operating conditions is often learned implicitly from data or treated as additional input features, rather than being embedded into a generative degradation-rate structure with explicit physical guidance. This may limit their extrapolation capability when the target cell operates under condition profiles that are different from those in the source data (Wang 2024a).

In contrast, model-based approaches characterize capacity degradation using stochastic models or state-space formulations motivated by physics or experience, and perform inference via parameter estimation or filtering to support online updating and lifetime assessment. Wang et al. (Wang 2024b) developed an improved Wiener-process degradation model with adaptive drift to capture degradation rate-volatility related effects, and validated on both laboratory battery and on-road EV battery. Zhang et al. (Zhang 2023a) propose a nonlinear Wiener-process degradation model with an Ornstein-Uhlenbeck dynamic covariate to capture time-varying operating conditions and improve RUL prediction accuracy on battery degradation data. These methods are appealing in reliability contexts due to their structured formulation and interpretability, yet a single parametric form may not be flexible enough to cover the diversity of degradation patterns induced by heterogeneous batteries and highly variable operating profiles, which can lead to model mismatch and reduced extrapolation accuracy (Zhang 2023b). From a reliability perspective, this motivates a practical need: learning transferable degradation regularities from diverse historical data, while adapting to the evolving operating conditions of a new cell to improve long-horizon capacity extrapolation.

To this end, this paper proposes a foundation-style lithium-ion battery degradation modelling framework that is adaptive to dynamic operating conditions. The key idea is to learn a shared generative degradation backbone from diverse historical cells and conditions, and to incorporate an operating-condition-aware physics guidance term to steer the degradation rate under varying conditions. The main contributions of this paper can be summarized as follows. (1) A foundation-style lithium-ion battery degradation model is developed, where transferable capacity degradation regularities are learned via a shared generative backbone, and cross-condition generalization is enhanced through an operating-condition adaptation mechanism. (2) A pre-training–adaptation–prediction pipeline is provided, leveraging diverse historical degradation data and enabling rapid personalization to a new cell from limited early-life observations, thereby supporting reliable capacity extrapolation and lifetime assessment in practical settings.

The remainder of this paper is organized as follows. Section 2 presents the model formulation, including the degradation foundation backbone and the operating-condition adaptation mechanism. Section 3 describes the learning objective and the pre-training and adaptation pipeline for capacity forecasting and RUL prediction. Section 4 reports the case study on lithium-ion batteries. Section 5 concludes the paper and outlines future work.

2. Model formulation

2.1. *Degradation Foundation Backbone*

In practice, the battery capacity is only observed after each charge–discharge cycle. We denote the discrete capacity observations as $y_0, y_1, \ldots, y_K$, where y_0 is the initial capacity and y_k is the capacity measured after the k-th cycle. These measurements form a degradation trajectory. Meanwhile, the battery operates under a time-varying operating-condition trajectory $c_0, c_1, \ldots, c_K$, where c_k collects the condition descriptors at cycle k. Our goal is to build a foundation backbone that can generate the degradation trajectory of the battery capacity as

accurately as possible under the given operating condition trajectory.

To this end, we model the latent degrading state $X(k)$ using a discrete-time Wiener-type stochastic evolution. Specifically, the backbone is written as

$$X(k+1)-X(k)=f_\theta\left(X(k),k,c_k\right)+\sigma_B\,\Delta B(k), \quad (1)$$

$$y_k=X(k)+\epsilon_k, \quad (2)$$

where the drift term $f_\theta\left(X(k),k,c_k\right)$ represents the capacity degradation rate at cycle k given the current state $X(k)$ and the current operating conditions c_k. We parameterize f_θ by a multilayer perceptron (MLP) to enhance the expressive power of the backbone and thereby better capture shared degradation patterns across different cells and operating profiles.

The term $\Delta B(k)$ denotes the increment of a standard Brownian motion over one cycle step, which is typically modelled as $\Delta B(k)\sim\mathcal{N}(0,1)$ after normalization of the discrete time step. The scalar $\sigma_B>0$ controls the magnitude of the process noise and quantifies the intrinsic stochasticity of degradation evolution. The measurement noise ϵ_k represents observation error in capacity readings; it is assumed to be zero-mean Gaussian, $\epsilon_k\sim\mathcal{N}\left(0,\sigma_\epsilon^2\right)$, with constant variance σ_ϵ^2 independent of k.

Under this formulation, the latent process $X(k)$ describes the underlying degradation progression, while y_k is the noisy capacity observation available in practice. This foundation backbone provides a flexible generative model that captures shared capacity degradation patterns while retaining stochasticity and measurement noise.

2.2. *Operating-condition Adaptation*

Although the backbone model above can learn shared degradation patterns from multiple cells, real lithium-ion batteries operate under highly heterogeneous and time-varying conditions, such as temperature, DOD, and C-rate. These operating conditions can substantially modulate the instantaneous degradation rate, meaning that a purely data-driven drift term may require excessive data to generalize across unseen condition trajectories. To incorporate such domain knowledge in a controllable and interpretable way, we augment the drift component with a physics-guided term f_p, which provides a quantitative reference for the capacity-fade rate under the current state, cycle index, and operating condition.

As a representative example, we consider an Arrhenius-type degradation relation that has been widely used to characterize how temperature and charge/discharge rate affect capacity loss in lithium-ion batteries (Chen 2024; Wang 2011). Specifically, the normalized capacity loss can be expressed as

$$Q_{loss}(t)=Ae^{-\left(\frac{E_a-B\cdot C_{rate}}{RT_a}\right)}\left(A_h\right)^z \quad (3)$$

where $Q_{\text{loss}}(t)$ denotes the normalized capacity loss at time t, E_a is the activation energy, C_{rate} is the charge/discharge rate, R is the gas constant, T_a is the absolute ambient temperature, A_h is the amp-hour throughput, and A, B, and z are degradation-related coefficients.

To align with the common practice that capacity is observed once per cycle, Eq. (3) is first differentiated w.r.t time, which yields an increment expression of the normalized capacity loss between *t* and *t*+1 (Song 2014):

$$Q_{loss}(t+1)-Q_{loss}(t)=\Delta A_h zA^{\frac{1}{z}}e^{-\left(\frac{E_a-B\cdot C_{rate}}{zRT_a}\right)}\times Q_{loss}(t)^{\frac{z-1}{z}}, \quad (4)$$

where ΔA_h is the amp-hour-throughput over [*t*,*t*+1], and I_b is the current.

Then, we adopt a standard engineering approximation that the capacity loss between inspections within one cycle is neglected, so that a single capacity value represents the capacity throughout cycle *k*. Next, we integrate the increment form over the time interval corresponding to the cycle *k*, and to connect the capacity loss formulation with the degrading state $X(k)$, we use the following relationship,

$$Q_{\text{loss}}(k)=\frac{X(0)-X(k)}{X(0)},$$

which allows the capacity loss from cycle k to k+1 to be expressed directly in terms of the state increment. Consequently, the physics-guided cycle-wise degradation rate can be written as

$$\begin{aligned} f_p\left(X(k),k,c_k\right) &= \left[Q_{\text{loss}}(k)-Q_{\text{loss}}(k+1)\right]X(0) \\ &= -X(0)\left(X(0)-X(k)\right)^{1-\frac{1}{z}} \\ &\quad \times DOD_k z\left(Q_{non}Ae^{-\left(\frac{E_a-B\cdot C_{rate,k}}{RT_{a,k}}\right)}\right)^{\frac{1}{z}} \end{aligned} \quad (5)$$

where $c_k=\left(DOD_k,T_{a,k},C_{\text{rate},k}\right)$ is the operating-condition vector for cycle k.

To realize that the model can better adapt to dynamic operating conditions while preserving the expressiveness of the foundation backbone, we next design a dedicated training objective that balances data fidelity with physics-informed regularization.

3. Model training and adaptation

3.1. *Learning Objective*

As a generative model, we train the proposed backbone by maximizing the probability of observing the capacity trajectory under the model. Given observations $y_{0:K}=\{y_0,\ldots,y_K\}$ and condition sequence $c_{0:K}=\{c_0,\ldots,c_K\}$, the maximum-likelihood objective can be written as

$$\begin{aligned} &\max_\theta \log p_\theta\left(y_{0:K}\,|c_{0:K}\right) \\ &=\max_\theta \sum_{k=0}^{K}\log p_\theta\left(y_k\,|y_{0:k-1},c_{0:k}\right). \end{aligned} \quad (6)$$

In addition, we would like the learned degradation-rate function f_θ to stay close to the physics-guided rate f_p. To this end, we introduce an ℓ_2 physics regularization via a Lagrange-multiplier-style penalty and obtain the following regularized objective:

$$\begin{aligned} &L(\theta,p)=\log p_\theta\left(y_{0:K}\,|c_{0:K}\right) \\ &-\lambda\sum_{k=0}^{K-1}\left\|f_\theta\left(X(k),k,c_k\right)-f_p\left(X(k),k,c_k\right)\right\|_2^2, \end{aligned} \quad (7)$$

where $\lambda>0$ controls the strength of the physics guidance, and $p=\{A,B,E_a,z\}$ represents learnable physical parameters. This objective is written for a single trajectory for clarity. It can be straightforwardly extended to a training set containing N trajectories $\left\{\left(y_{0:K_n}^{(n)},c_{0:K_n}^{(n)}\right)\right\}_{n=1}^{N}$ as

$$\begin{aligned} &L(\theta,p)=\sum_{n=1}^{N}\log p_\theta\left(y_{0:K_n}^{(n)}\,\middle|c_{0:K_n}^{(n)}\right) \\ &-\lambda\sum_{n=1}^{N}\sum_{k=0}^{K_n-1}\left\|\begin{matrix} f_\theta\left(X^{(n)}(k),k,c_k^{(n)}\right) \\ -f_p\left(X^{(n)}(k),k,c_k^{(n)}\right)\end{matrix}\right\|_2^2 \end{aligned} \quad (8)$$

Under the common assumption of additive Gaussian observation noise, the first term in the objective is equivalent to a sum of squared errors between the generated latent trajectory and the observations,

$$\log p_\theta\left(y_{0:K}\,|c_{0:K}\right)\propto-\sum_{k=0}^{K}\left\|y_k-X(k)\right\|_2^2,$$

which indicates that evaluating the first term requires generating the latent path $X(k)$. Meanwhile, the second term also depends on the same latent path through $f_\theta\left(X(k),k,c_k\right)$ and $f_p\left(X(k),k,c_k\right)$. Although the objective involves stochastic sampling of Brownian increments during path generation, prior studies (Li 2020) have shown that the resulting optimization problem remains differentiable with respect to the parameters, enabling end-to-end training via backpropagation.

In the next section, we present the overall workflow for pre-training this foundation-style degradation model on diverse historical cells with varying conditions and then adapting it to a new cell for prognostics.

3.2. *Pre-training and Adaptation Pipeline*

Given multi historical capacity degradation trajectories with their operating-condition sequences, we first pre-train a shared degradation backbone to capture condition-aware yet transferable degradation patterns. For a new cell, we then adapt the model using only its partial trajectory up to the current cycle and generate the future capacity trajectory conditioned on future operating conditions. In

practice, when future conditions are unavailable, we approximate them by the empirical average of the observed conditions for that cell.

To translate capacity forecasting into lifetime prognostics, we define the RUL through the first-hitting time (FHT). Starting from the current state, the FHT is the first cycle when the latent degradation process crosses a predefined degradation threshold ξ, i.e.,

$$\tau^{(s)} = \inf\{t > k : X(t) \le \xi\} \tag{9}$$

We estimate the RUL distribution by simulating multiple future paths from the adapted model, collecting the corresponding FHT samples, and fitting a parametric distribution to obtain both point estimates and uncertainty quantification. Based on the above description, the overall procedure can be summarized in Algorithm 1.

Algorithm 1. Pre-training and Adaptation Pipeline for capacity forecasting and RUL prediction

Input: Historical dataset: $\mathcal{D}_{\text{hist}} = \left\{\left(y_{0:K_i}^{(i)}, c_{0:K_i}^{(i)}\right)\right\}_{i=1}^{N}$, new cell partial data $(y_{0:k}^{\text{new}}, c_{0:k}^{\text{new}})$, failure threshold ξ.

Output: Forecasted capacity sequence $\hat{y}_{k+1:k+H}^{\text{new}}$ and estimated RUL distribution $\hat{p}\left(\text{RUL}\middle| y_{0:k}^{\text{new}}, c_{0:k}^{\text{new}}\right)$.

1 **Initialize.** Initialize shared backbone parameters θ and physics parameters p.

2 **Pre-training on historical data.** Train (θ, p) on $\mathcal{D}_{\text{hist}}$ by maximizing the proposed learning objective (8). Update parameters by Adam until convergence.

3 **Adaptation.** Fine-tune parameters on $(y_{0:k}^{\text{new}}, c_{0:k}^{\text{new}})$ using the same learning objective (7), optionally with early stop and small learning rate to avoid overfitting.

4 **Future operating-condition approximation.** If future conditions are unavailable, set a constant proxy profile $\bar{c}^{\text{new}}$ as the empirical mean of $c_{0:k}^{\text{new}}$, and form future conditions $c_{k+1:k+H}^{\text{new}} \leftarrow \bar{c}^{\text{new}}$.

5 **Capacity forecasting.** Using the adapted model and $c_{k+1:k+H}^{\text{new}}$, generate the forecasted trajectory $\hat{y}_{k+1:k+H}^{\text{new}}$.

6 **FHT-based RUL sampling**. For $s = 1,\ldots,S$: simulate a future latent path from the adapted model starting at cycle k, obtain the FHT by Eq. (9), and record $\text{RUL}^{(s)} = \tau^{(s)} - k$.

7 **RUL distribution fitting.** Fit a distribution $\hat{p}(\text{RUL})$ to $\{\text{RUL}^{(s)}\}_{s=1}^{S}$.

8 **Return.** Output $\hat{y}_{k+1:k+H}^{\text{new}}$ and $\hat{p}\left(\text{RUL}\middle| y_{0:k}^{\text{new}}, c_{0:k}^{\text{new}}\right)$.

Through the above pipeline, the proposed framework learns transferable degradation regularities from diverse historical batteries and operating conditions, and can be rapidly adapted to a new cell using only a short early-life record, thereby producing both future capacity trajectory forecasts and RUL prediction. Fig. 1 gives the framework of the proposed method.

The next section presents a case study to demonstrate its accuracy and applicability on lithium-ion battery data.

4. Case study

4.1. *Comparative Models and Metrics*

To demonstrate the superiority of the proposed method, the following Wiener-type models that can consider the influence of operating conditions are selected for comparison:

M1 (Yan 2020): a linear Wiener process model considering degradation rate-volatility relative effect.

M2 (Kong 2022): a nonlinear Wiener process model that uses a power function as a shape function.

M3 (Liu 2022): a nonlinear Wiener process model that uses an MLP as a shape function.

For convenience, the three comparative models are expressed as the following differential forms, respectively,

$$\text{M1}: \Delta X(k) = \lambda(c_k) + \kappa\sqrt{\lambda(c_k)}\,\Delta B(k) \tag{9}$$

$$\text{M2}: \Delta X(k) = \lambda(c_k) \times abk^{b-1} + \sigma\Delta B(k) \tag{10}$$

$$\text{M3}: \Delta X(k) = \lambda(c_k) \times \text{MLP}(k) + \sigma\Delta B(k) \tag{11}$$

where $\lambda(c_k)$ is an Arrhenius-type empirical physics formula. In this case study, $\text{MLP}(k)$ and f_θ are both parameterized by MLPs with two hidden layers and a softplus activation. The hidden size is 64. In the implementation, the regularization coefficient λ is controlled by a linear warm-up scheduler and is gradually increased during the first 1000 training iterations,

rather than being fixed from the beginning. S is set to be 15 in this study.

4.2. *Application to Lithium-ion Battery Data*

To evaluate the proposed approach under realistic, time-varying operating conditions, we conduct a case study on CycleLife-SJTUIE, a publicly available lithium-ion battery degradation dataset collected on our experimental platform. The dataset contains eight LFP/graphite cells with a nominal capacity of 13 Ah, tested indoors without active temperature control and cycled using a battery tester. The cells are divided into two groups, each following a different charge-discharge configuration to induce distinct operating-condition profiles. Further details on the tested cells, experimental setup, and cycling protocols are provided in (Wu 2025). Fig. 2 summarizes representative trajectories, including the capacity degradation, temperature evolution, and charging profiles observed during the tests.

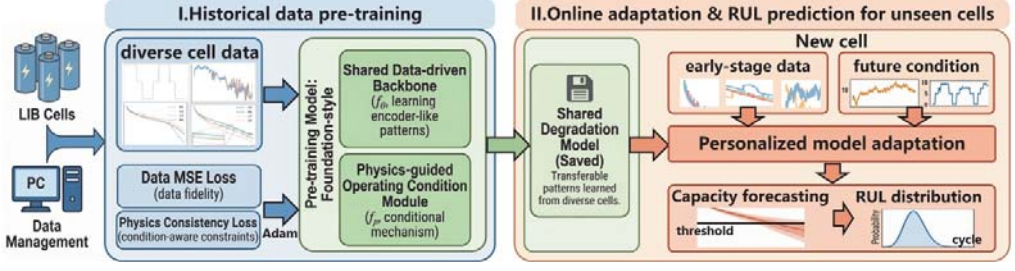

Fig. 1. The framework of the proposed method.

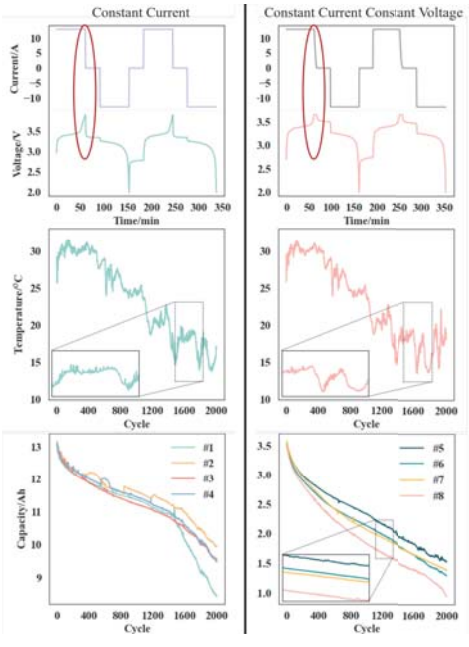

Fig. 2. The charging profiles, temperature evolution and capacity degradation for two configurations.

Cells #1, #3, #7, and #8 are treated as historical batteries for pre-training the degradation backbone, while the remaining cells are regarded as new cells for adaptation and subsequent evaluation of capacity forecasting and RUL prediction. First, the capacity forecasting performance of each method for new cells is evaluated on mid-term and long-term extrapolation, which refers to continuously predicting 400 cycles and 1600 cycles, respectively. The accuracy is measured by the MSE between the predicted and true capacity trajectories, averaged over cycles and cells. The results are summarized in Fig. 3.

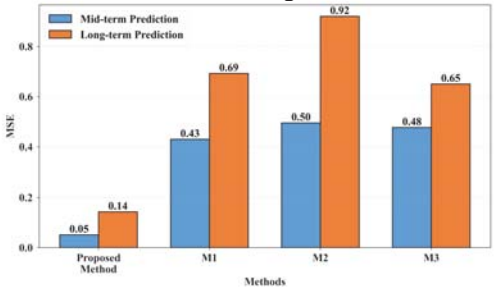

Fig. 3. The comparative results of mid-term and long-term prediction.

From Fig. 3, the proposed method consistently achieves the lowest MSE in both mid-term and long-term prediction. It indicates that the proposed method not only predict capacity degradation more accurately in the mid horizon, but also remains a clear advantage

under the more challenging long-horizon prediction task, demonstrating stronger generalization and more reliable long-term forecasting performance. For the task of RUL prediction, the early 500-cycle data of each new cell are used for adaptation. The accuracy of RUL prediction is evaluated every 20 cycles after the adaptation stage. Table I provides the relative errors (RE) between the expected predicted value and true value at the stages when remaining 60%, 40%, and 20% lifetime for each cell.

It can be seen from Table I that the proposed method has the smallest error in most stages, with REs mostly within ±10% and not exceeding about ±20% in magnitude, indicating good accuracy and limited bias. In contrast, M1 and M3 exhibit systematic underestimations for all cells, suggesting poor calibration throughout the lifetime. M2 shows mixed behaviour. It can be competitive at early stages for some cells, but its errors grow dramatically as the RUL decreases, with severe overestimation in several cases. These results demonstrate that the proposed approach is more reliable and stable than other methods in RUL prediction at different cells and life stages.

To further comprehensively compare these methods, some metrics including MAE, RMSE, LMSF, MAPE and MSPE are deployed for evaluating overall cell-level performance of RUL prediction, whose definitions can be referred to (Chen 2024). The normalized results are shown in Fig. 4 in form of wind rose diagram.

Obviously, Fig. 4 shows that the proposed method is optimal in all metrics for each cell, demonstrating superior overall performance in RUL prediction. All the above provided comparative results confirm that our approach provides accurate and robust degradation modeling and RUL prediction on new cells under varying operating conditions.

Table 1. Relative errors of RUL prediction of RUL prediction at representative lifetime

RE(%) / Method	#2			#4			#5			#6		
	60%	40%	20%	60%	40%	20%	60%	40%	20%	60%	40%	20%
The proposed	-7.33	+8.71	-0.41	-13.2	-11.1	+3.15	-14.8	-15.0	-19.6	-10.9	-5.89	-2.14
M1	-53.3	-45.2	-49.8	-44.6	-43.2	-34.1	-56.8	-56.9	-59.2	-54.4	-51.7	-49.8
M2	-6.98	+27.3	+82.9	+6.41	+36.4	+115	-25.0	-4.39	+37.7	-17.4	+8.07	+62.0
M3	-73.3	-68.7	-71.4	-69.6	-68.9	-63.9	-61.0	-61.1	-63.2	-63.8	-61.7	-60.2

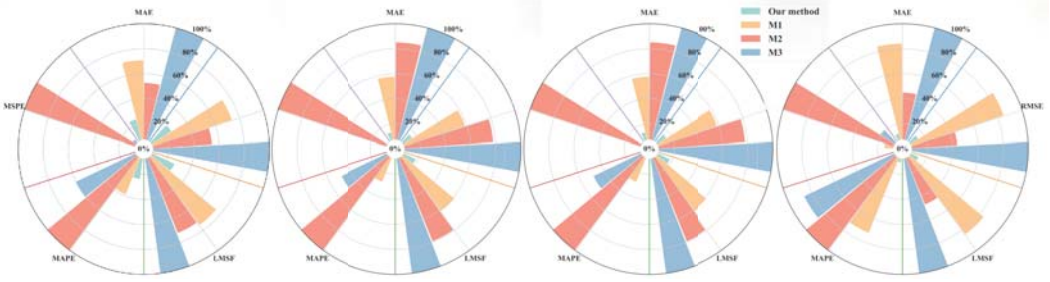

(a) Cell #2 (b) Cell #4 (c) Cell #5 (d) Cell #6

Fig. 4. The wind rose chart of the five metrics for each model at each cell.

5. Conclusion

In this paper, a foundation-style degradation modelling framework is proposed. It contains a Wiener-type degradation backbone that learns shared degradation patterns from historical trajectories and operating-condition adaptation mechanism that can make the model adapt to a new cell with varying operating conditions by introducing physical guidance. The framework is able to learn physically meaningful degradation rate under dynamic conditions without reducing modelling expressiveness. Then, the corresponding training and adaptation procedure is established to provide capacity forecasting and RUL prediction of new cells. The practical effectiveness of the proposed framework is validated by experiments on our lab dataset

CycleLife-SJTUIE. The results demonstrate reliable adaptation and stable performance across varying test cells and operating conditions, indicating a possible pathway toward reliable prognostics in engineering deployments.

Future work will further explore scenario-based RUL prediction under uncertain future usage profiles by incorporating multiple possible operating-condition trajectories instead of relying only on the empirical-mean approximation.

Acknowledgement

This work was supported by National Natural Science Foundation of China under Grant 72571178, Grant 72471143.

References

Chen, Z., Wang, Z., Wu, W., Xia, T., and Pan, E. (2024). A Hybrid Battery Degradation Model Combining Arrhenius Equation and Neural Network for Capacity Prediction under Time-Varying Operating Conditions. Reliability Engineering & System Safety 252: 110471.

Guirguis, J., Abdulmaksoud, A., Ismail, M., Kollmeyer, P. J., and Ahmed, R. (2024). Transformer-Based Deep Learning Strategies for Lithium-Ion Batteries SOX Estimation Using Regular and Inverted Embedding. IEEE Access 12: 167108–19.

He, J., and Wu, L. (2023). Cross-Conditions Capacity Estimation of Lithium-Ion Battery with Constrained Adversarial Domain Adaptation. Energy 277: 127559.

Kong, J.-Z., Wang, D., Yan, T., Zhu, J., and Zhang, X. (2022). Accelerated Stress Factors Based Nonlinear Wiener Process Model for Lithium-Ion Battery Prognostics. IEEE Transactions on Industrial Electronics 69 (11): 11665–74.

Li, X., Wong, T.-K. L., Chen, R. T. Q., and Duvenaud, D. (2020). Scalable Gradients for Stochastic Differential Equations. Proceedings of the Twenty Third International Conference on Artificial Intelligence and Statistics, June 3, 3870–82.

Li, Y., Li, L., Mao, R., Zhang, Y., Xu, S., and Zhang, J. (2024). Hybrid Data-Driven Approach for Predicting the Remaining Useful Life of Lithium-Ion Batteries. IEEE Transactions on Transportation Electrification 10 (2): 2789–805.

Liu, D., Wang, S., and Zhang, C. (2022). Reliability Estimation from Two Types of Accelerated Testing Data Based on an Artificial Neural Network Supported Wiener Process. Applied Mathematics and Computation 417: 126757.

Patrizi, G., Martiri, L., Pievatolo, A. (2024). A Review of Degradation Models and Remaining Useful Life Prediction for Testing Design and Predictive Maintenance of Lithium-Ion Batteries. Sensors 24 (11): 3382.

Severson, K. A., Attia, P. M., Jin, N. (2019). Data-Driven Prediction of Battery Cycle Life before Capacity Degradation. Nature Energy 4 (5): 383–91.

Song, Z., Li, J., Han, X. (2014). Multi-Objective Optimization of a Semi-Active Battery/Supercapacitor Energy Storage System for Electric Vehicles. Applied Energy 135: 212–24.

Wang, F., Zhai, Z., Zhao, Z., Di, Y., and Chen, X. (2024a). Physics-Informed Neural Network for Lithium-Ion Battery Degradation Stable Modeling and Prognosis. Nature Communications 15 (1): 4332.

Wang, J., Liu, P., Hicks-Garner, J. (2011). Cycle-Life Model for Graphite-LiFePO4 Cells. Journal of Power Sources 196 (8): 3942–48.

Wang, Z., Chen, Z., Xia, T., and Pan, E. (2024b). Degradation Modeling Considering the Dependency of Rate and Volatility for Real-Time Prognostics With Error Correction. IEEE Transactions on Instrumentation and Measurement 73: 1–12.

Wu, W., Chen, Z., Liu, W., Zhou, D., Xia, T., and Pan, E. (2025). Battery Health Prognosis in Data-Deficient Practical Scenarios via Reconstructed Voltage-Based Machine Learning. Cell Reports Physical Science 6 (2): 102442.

Yan, B., Ma, X., Yang, L., Wang, H., and Wu, T. (2020). A Novel Degradation-Rate-Volatility Related Effect Wiener Process Model with Its Extension to Accelerated Ageing Data Analysis. Reliability Engineering & System Safety 204: 107138.

Zhang, S., Zhai, Q., Shi, X., and Liu, X. (2023a). A Wiener Process Model With Dynamic Covariate for Degradation Modeling and Remaining Useful Life Prediction. IEEE Transactions on Reliability 72 (1): 214–23.

Zhang, Y. (2023b). Joint Nonlinear-Drift-Driven Wiener Process-Markov Chain Degradation Switching Model for Adaptive Online Predicting Lithium-Ion Battery Remaining Useful Life. Applied Energy.

Zhao, J., Zhu, Y., Zhang, B. (2023). Review of State Estimation and Remaining Useful Life Prediction Methods for Lithium–Ion Batteries. Sustainability 15 (6): 5014.

Zubi, G., Dufo-López, R., Carvalho, M., and Pasaoglu, G. (2018). The Lithium-Ion Battery: State of the Art and Future Perspectives. Renewable and Sustainable Energy Reviews 89: 292–308.